JOURNAL OF ENERGY SYSTEMS

2024, 8(1)

2602-2052 DOI: 10.30521/jes.1362581 Research Article

Demagnetization effects of surface-mounted permanent magnet synchronous wind generator

Adem Dalcalı*
Bandırma Onyedi Eylül University, Bandırma, Balıkesir, Türkiye, adalcali@bandirma.edu.tr
Erol Kurt
Gazi University, Ankara, Türkiye, ekurt@gazi.edu.tr

Submitted: 18.09.2023
Accepted: 01.12.2023
Published: 31.03.2024

* Corresponding Author

Abstract: To prevent fossil resources from being depleted and protect the natural balance, renewable resources come to the forefront as an alternative to fossil resources. Wind energy resources, among the renewable energy resources, are important in terms of ensuring the reliability of energy and the use of their resources. Generators are the most important components for the conversion of wind power. Permanent magnet synchronous generators (PMSGs) are preferred in wind turbines since they have high efficiency and high volume/torque densities, thereby optimization of the PMSGs is an important topic for the wind energy community. On the one hand, these machines can cause problems due to overheating and mechanical friction during their long-time operation. To identify the performance lack of the machines due to the de-magnetization faults, systematic work has been performed. When a magnet of a PMSG is de-magnetized at different rates (i.e. 33%, 50%, and 100%), we have explored the artifacts in the electric generation. Besides, the torque performances of the generator at rated load are examined and the flux density distributions are revealed. The rated torque decreased substantially when the demagnetization rate of the magnet increased.

Keywords: *Finite element analysis, Partial demagnetization, Permanent magnet synchronous generator, Wind energy*

Cite this paper as: Dalcalı, A., & Kurt, E. Demagnetization effects of surface-mounted permanent magnet synchronous wind generator. *Journal of Energy Systems 2024; 8*(1): 63-74, DOI: 10.30521/jes.1362581

1. INTRODUCTION

Ensuring the security of electrical energy supply is of critical importance. The destruction caused in fossil fuels and the decrease in known-reserves turn this situation into an even more difficult problem. Furthermore, increasing population and energy demand adversely affect the security of supply. Nowadays, the most important approach for the energy security is the diversification of the resources even for renewables. In this respect, renewable resources may be an important alternative both to meet the increasing energy demand and reduce the damages to nature due to conventional fuels. Renewable energy is known as the energy that renews itself over time although it may include a Carbon foot-print in some extend in the production scheme of its components. Renewable energy is al-so a local solution and is an environmentally friendly and fuel-free energy compared to the conventional methods. With the use of renewable resources, it is possible to reduce emissions caused by fossil fuels and ensure the effective use of countries' own resources. Solar, wind, hydroelectric, biomass, and geothermal resources can be indicated as the main renewable energy sources [1,2].

Wind energy among the other renewable resources plays a significant role in ensuring supply security and reducing external dependency, particularly for countries with windy regions. Wind energy is an environmentally friendly and rapidly growing type of energy that does not cause greenhouse gas emissions [3,4]. Especially with advancements in turbine control and production technologies, this rapid growth continues. This growth is also effective in enabling wind energy to produce electricity at a cost competitive with sources like coal or nuclear [5]. Electricity generation from wind energy can be performed a wide power scale from micro-Watts to giga Watts. Generators are among the most important components of wind turbines. Generators are used in many different structures in electricity generation from wind energy. Permanent Magnet Synchronous Generators (PMSGs) are widely used in parallel with the developing material technology [6]. The rotor magnetic field of PMSGs is formed by permanent magnets. Permanent magnets can be grouped as Alnico, ceramic (or ferrite), and rare-earth magnets. Advancements in materials and production technologies have increased the use of rare-earth magnets. Different shapes of magnets can be constructed for individual machines. They are especially preferred in applications where high-power density is required [7,8]. In any machine, operating environments, climatic conditions and mechanical frictions can yield to some problems in the machines. Especially their continuous long operating periods in harsh environmental conditions can cause various faults in machines. In general, these faults can be classified as magnetic, mechanical, and electrical faults. Brush-collector assembly fault, short-circuit ring fault, rotor bar fault, and magnet breakage fault may occur in the rotor part, depending on the type of machine [9]. Faults will of course affect the machine’s performance and reliability during the energy conversion.

In the literature, there are various fault detection and solution proposals for electrical machines. For instance, in the studies of Faiz and Nejadi-Koti, demagnetization errors occurring in Permanent Magnet Synchronous Motors (PMSMs) and diagnosis methods of these errors have been discussed [10]. The advantages, disadvantages, uncertainties of the techniques, and solutions to these uncertainties have been presented. In the study demagnetization faults have been indexed as current-based, voltage-based, torque-based, and magnetic flux-based [10]. Demagnetization faults of the PMSM under nonstationary conditions have been detected using time-frequency wavelet-based methods. Current harmonics have been detected in the analyses to identify the harmonics caused by demagnetization [11]. In another study focusing on the analysis of current harmonics, harmonics have been analyzed using Fast Fourier Transform (FFT) for the PMSM at nominal torque. Detection of demagnetization faults for any speed range has been achieved through analyses at different speeds [12].

In recent years, Neural Networks (NN) have been employed in motor fault detection [13-14]. Permanent magnet faults have been detected based on time-frequency domain analysis using short-time Fourier analysis of the stator current signal. Machine learning-based fault classification has been performed in

the study [15]. Similarly, a convolutional NN model has been proposed for detecting permanent magnet faults using the current signal. Experimental studies conducted on a designed PMSM have determined that convolutional NN yield successful results in fault diagnosis [16]. In another study employing the same method, the network was trained using the transfer learning technique, and the current signal obtained from FEA was utilized [17]. However, in studies utilizing artificial intelligence techniques, effective training of the network is crucial to achieve accurate results. Therefore, a large dataset is required for training. In a voltage-based study, an online method has been proposed for the detection of demagnetization faults. The proposed methodology is based on monitoring the zero-sequence voltage component of the stator phase voltage [18].

The Finite Element Method (FEM) is an effective technique used for possible fault detections. This method allows for various combinations of analyses. The impact of single magnet demagnetization in PMSMs has been investigated in series and parallel connected stator winding configurations. In the analyses, it was found that the induced emf value for the demagnetization of a single magnet decreases in series-connected winding generators [19]. In another application of FEM, local demagnetization fault of the PMSM has been studied using the magnetic equivalent circuit model. The magnetic leakage signal on the motor surface has been used as a fault signal in these analyses [20]. The signal analysis of faulty and healthy motor currents of an external rotor permanent magnet synchronous machine has been used for demagnetization fault detection. In the proposed method for the detection, a developed magnetic equivalent circuit is adopted and the results are com-pared with FEM analyses. The proposed method has been noted to have a shorter processing time compared to FEM [21]. FEM analysis has been employed to examine uniform and non-uniform irreversible demagnetization faults of a permanent magnet generator at different rates. Correlations have been established between faults defined by current harmonics and the analysis results [22]. Vibration analysis can also be used for demagnetization fault detections. In a study, for this purpose, a portion of the magnet has been transformed into a non-magnetic material for analysis. It is determined that the amplitudes of certain vibration components are proportional to the demagnetization level of the permanent magnets [23].

In the present study, we have considered a different machine with a 14-pole internal rotor, surface-mounted permanent magnet synchronous generator with a rated power of 2.5 kW. The fault analyses of the machine designed for wind turbines are conducted in different partial demagnetization status. In the analyzes, the induced torque and voltage waveforms are determined by demagnetizing a magnet selected in the rotor at different rates. The paper is organized as follows: In Section 2, the generators used in wind turbines and their characteristics have been examined. Subsequently, the dimensions and cross-sectional view of the designed PMSG have been provided. In the next section, faults and demagnetization faults in electrical machines are examined. In Section 4, comparative FEM results are presented in detail. Finally, the concluding remarks are reported in the last section.

2. GENERATORS FOR WIND TURBINES

Generators are electrical machines converting mechanical energy into electrical energy with minimum loss. Generators are among the most important components of wind turbine systems. Many generator models are used in different structures in wind turbines. Factors such as the presence of a gearbox, economic constraints, location selection, and power level affect the generator selection for different applications. Since direct-current (DC) generators have a brush-collector assembly, there is a disadvantage of difficulty in maintenance and frequent maintenance. DC generators are especially preferred in low power and grid-free applications. However, in asynchronous generators, this disadvantageous situation is not in question. But their low torque density and relatively low efficiency are their negative aspects, especially when compared to machines with magnets. Furthermore, the reactive power requirement of asynchronous generators and the need for a capacitor bank for this are important requirements. Asynchronous generators can be produced in two different types as wound rotor generators and squirrel cage rotor generators. The synchronous generators consist of a three-phase stator

and a magnet or wound rotor [24,25,26,27]. In synchronous generators, salient pole synchronous generators can be preferred especially in high pole applications, while permanent magnet synchronous generators can be preferred for high efficiency and power density requirements [28,29]. Fig. 1 shows the detailed structure of turbine systems.

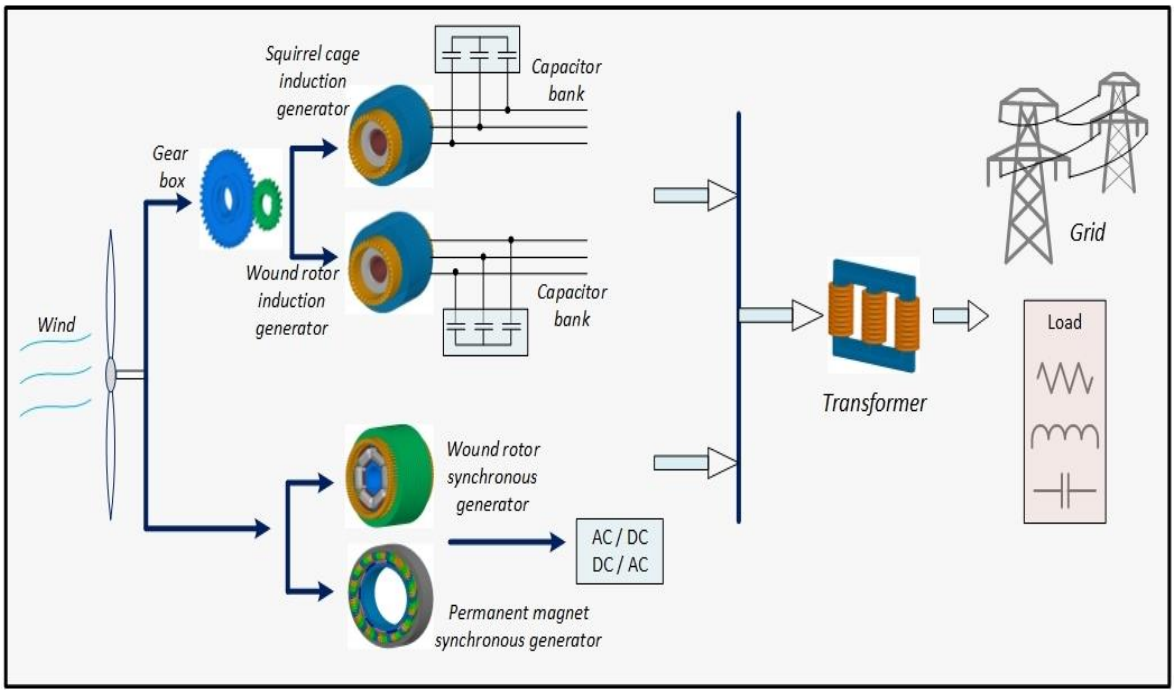

Figure 1. Generator systems used in wind turbines.

The comparison of wind turbines in terms of excitation, torque density and efficiency are summarized in Table 1 [30].

Table 1. Comparison of generators according to Ref. [30]. (NR: Not Required, L: Low, M: Middle, H: High).

Type	Excitation	Torque density	Efficiency
DC	DC	L	M
Asynchronous	NR	L	M
Synchronous	DC	M	M
PM synchronous	NR	H	H

In terms of cost, when evaluated, DC machines are high in both maintenance and production costs due to the brush-commutator arrangement. Asynchronous generators are cost-effective both in production and operation. On the other hand, PM synchronous generators have a high production cost depending on the magnet material used, while maintenance costs are moderate.

2.1. Designed PMSG

The widespread use of Neodymium-Iron-Boron magnets and improvements in drive technology have enabled permanent magnet machines to be frequently preferred, especially for low-speed and variable-speed applications. In these machines, different magnet materials and geometrical structures affect the machine's performance. PMSGs are machines with easy manufacturing, low torque ripple, and high-power density. The absence of windings on the rotor and, therefore, no rotor copper loss results in high efficiency. Permanent magnet generators can be directly connected to wind turbines without the need for a gear system and can be designed with either axial or radial flux [31,32]. Magnets can be mounted on the surface or have an interior structure. While the interior type is preferred especially at high speeds, the surface-mounted structure can be preferred for an effective air gap. The design of electrical machines begins with the equation given in Eq. 1, referred to as the sizing equation [33,34].

$$S = 11\, k_w\, \bar{B}\, ac\, D^2 L\, n \qquad (1)$$

In the above equation, S is the power in VA, k_w is the winding factor, $\bar{B}$ is the specific magnetic loading, ac is the specific electrical loading. $\bar{B}$ and ac values are determined by the machine designer. In the equation, D is the generator's diameter and L is the axial length are determined in meters. The performance of the generator can be improved by the correct selection of the speed of the machine and the electrical and magnetic loading. The volume of the generator is related to D^2L and is inversely proportional to the speed. Practically, the synchronous speed is determined by the number of poles and the frequency. The specific electrical loading value is defined as the ampere-conductor value per unit circumference in the air gap of the stator. When selecting this value, operating voltage, synchronous reactance, short circuit current, copper loss and temperature rise should be taken into account. In a 3-phase generator, the specific electrical load is determined by Eq. 2 [33, 34] chosen.

$$ac = \frac{6\, I\, N}{\pi\, D} \qquad (2)$$

In the equation, I is the phase current and N is expressed as turns/phase. In determining the specific magnetic loading, iron losses, temperature rise, short circuit current and parallel connection of the generator should be taken into account. Table 2 contains the specifications of the generator subject to the study.

Table 2. Specifications of the designed generator.

Parameter	Value	Parameter	Value
Stator / Rotor OD (mm)	280 / 198.4	Skew	0
Stator / Rotor Inner Diameter (mm)	202 / 164	Embrace	0.75
Axial Length (mm)	54	Offset (mm)	0
Magnet Thickness (mm)	5.4	Stator / Rotor material	M470
Number of Poles / slots	14 / 84	Magnet Material	N35

Fig. 2 shows the 3D model and mesh structure of the designed generator.

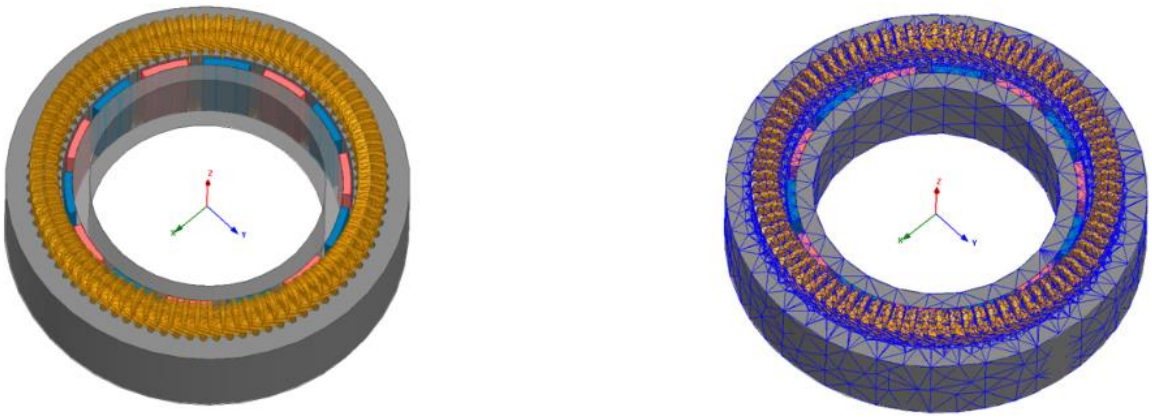

Figure 2. PMSG model with mesh structure.

3. DEMAGNETIZATION FAULT

The use of electrical machines in the industry is increasing day by day. The production of high-efficiency electric machines has been achieved through the advancement of material and electronic technology. However, the operating environment conditions and frequency of operation of these machines can affect their performance and lead to faults during operation. Particularly, disruptions in critical tasks such as

healthcare, defense, etc., can result in loss of life and property. Mechanical, thermal, electronic and material-based faults can be encountered in electrical machines. Although there are different error classifications in permanent magnet machines, they can be summarized as in Fig. 3 [35,36].

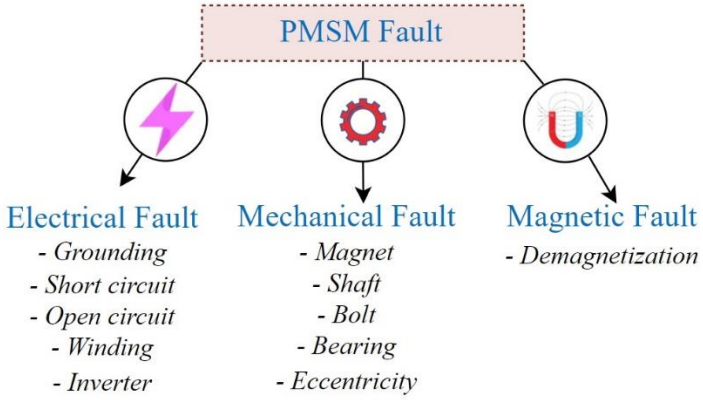

Figure 3. Main faults encountered in permanent magnet machines.

The permanent magnets provide the magnetic energy that they store to the circuit continuously. Ideally, permanent magnets have a high demagnetizing force and permanent magnetism. Furthermore, permanent magnets are rigid magnetic materials with large hysteresis loops. Many different magnet materials are used in practice. Alnico, Samarium-Cobalt (SmCo), Neodymium-Iron-Boron (NdFeB), and ferrite alloys are currently commercially used world-widely [37]. Permanent magnet machines are frequently preferred in industrial applications due to their high efficiency, high power/weight ratio, and high flux density advantages [38]. For a comparison of magnets, BH_{max}, the product of permanent magnetism and coercive force, is often used. The magnetic field provided by the magnet becomes stronger with the increase in this value. Table 3 contains the magnetic and thermal properties of some commercially used magnets [37,39,40].

Table 3. Magnetic properties of magnets.

Material	B_r(T)	H_c(kA/m)	BH_{max}(kJ/m^3)	Max. operating temperature (°C)	Curie temperature (°C)
Ferrit	0.4	240	27-35	300	450
Alnico	1.1	130	75-80	500	830
SmCo	0.97	750	130-190	250	720
NdFeB	1.20	870	200-290	140	310

SmCo and NdFeB magnets possess a linear demagnetization curve, high remanence, and high energy production capability. These features have led to an increase in the usage of these types of magnets in high-power density applications. In addition to the materials in the table, the process of producing different components and magnets and improving their performance continues with the help of developing magnet production technology. As is known, losses emerge in electric machinery during operation, and these losses occur in the form of heat. As stated in Table 3, there are certain thermal limits for the operation of magnets. This heat adversely affects the performance of permanent magnets. Additionally, magnets are very hard and brittle. Considering the operating conditions and these dis-advantageous conditions of magnets, demagnetization may occur in magnets. Demagnetization faults that occur in permanent magnet machines take an important place in these machines. Demagnetization can occur, especially in cases where a high torque requirement is necessary. In these situations, the magnetic field generated by the stator current is an opposing magnetic field to the magnetic field produced by the magnet, which can cause the magnet to demagnetize. Additionally, an increase in temperature during operation or incorrect heat distribution can also lead to the formation of demagnetization [11]. When demagnetization occurs, the value of the stator rated current increases to achieve the same output torque. Therefore, demagnetization leads to an increase in copper loss and a rise in the temperature of the permanent magnet machine [18]. Demagnetization can occur in all or part of the magnet [41]. In the examination of the demagnetization effect, analyses can be performed using parameters such as back EMF, torque, current, volt-age signal, and cogging torque. Additionally,

temperature analysis, vibration analysis, acoustic noise analysis, electromagnetic analysis, and infrared diagnostics can also be utilized in diagnosing this fault [12,42,43]. Demagnetization faults can be determined by many different methods [44]. They can be determined directly by a Hall sensor [45] or artificial intelligence techniques [46].

4. FEM ANALYSIS OF PMSG

In order to provide the desired performance, mechanical, thermal, and material problems need to be evaluated together. Under the determined constraints, many different explorations are needed to reach a design with the desired cost and efficiency values. All these designs and analyses involve time-consuming processes. Mathematically based methods are used to solve such problems. The use of methods like finite differences and finite elements, along with computer software, is effective in reaching a solution [47]. Among these methods, the FEM is used in a wide range of applications, including electric machinery [48], the healthcare sector [49], and the automotive industry [50]. FEM is used in the solution of quantities that can be expressed by partial differential equations in a certain region. The determined region is divided into a finite number of small regions. The contributions of the elements surrounding the region are chained together. The desired sizes are obtained by solving this chain equation set. By applying FEM to the generator, the performance parameters of the generator, such as flux distribution, losses, efficiency, and induced voltage waveform, can be obtained [47]. In the study, different rates of breakage of the determined magnet are considered as magnet fault. Fig. 4 displays the structures created. In the first model, there is no fault in the magnet (Fig. 4(a)). In the model in Fig. 4(b), 1/3 of the magnet is broken, while 1/2 is broken in the structure in Fig. 4(c). In the structure in Fig. 4(d), the magnet was completely removed since it was assumed that the magnet was completely broken.

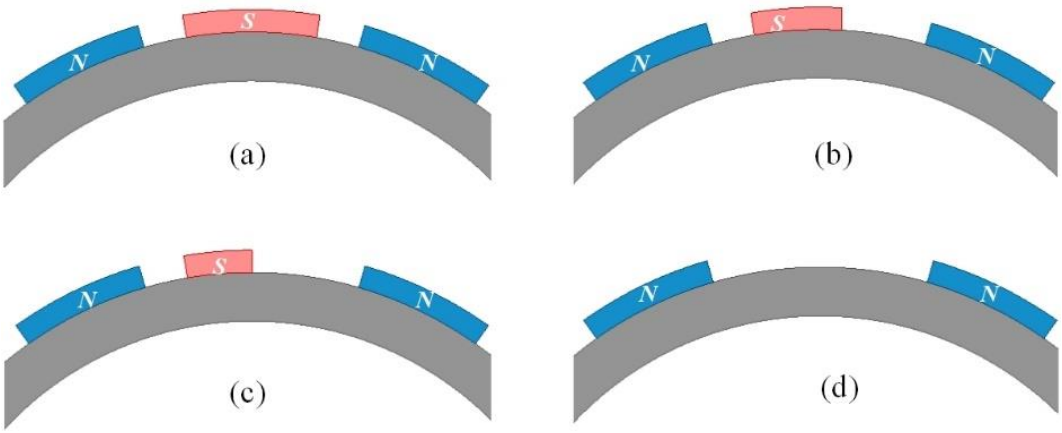

Figure 4. Magnet structures: a) healthy model, b) 1/3 broken structure, c) 1/2 broken structure, and d) all broken.

Obtaining the magnetic field distribution is important in extracting the operational performance of generator. Magnetic flux densities were acquired by applying FEA to these four different structures created. In the model designs, the magnetic field can be expressed using one of Maxwell's Equations [47].

$$\nabla \times \vec{E} = -\frac{\partial B}{\partial t} \tag{3}$$

In the equation, $\vec{E}$, represents the electric field intensity, $\vec{B}$, denotes the magnetic flux density. The magnetic vector potential $\vec{A}$ in terms of magnetic flux density:

$$\vec{B} = \nabla \times \vec{A} \tag{4}$$

Due to the nonlinearity of the *BH* characteristic of the ferromagnetic core material used, the variable permeability is denoted as $v = \frac{\partial B}{\partial H}$, where the magnetic vector potential:

$$\nabla \times \left(v \nabla \times \vec{A}\right) = \vec{J} \tag{5}$$

In Fig. 4, the magnetic flux density distributions and the state of the magnetic flux lines are given at rated load in the cross-sectional area. The magnetic flux density distribution provided in Fig. 5 can be determined using the equations given by Eqs. 6 and 7, as shown below.

$$\frac{\partial}{\partial \mathrm{x}}\left(v\frac{\partial A}{\partial x}\right)\boldsymbol{x} + \frac{\partial}{\partial \mathrm{y}}\left(v\frac{\partial A}{\partial y}\right)\boldsymbol{y} + \frac{\partial}{\partial \mathrm{z}}\left(v\frac{\partial A}{\partial z}\right)\boldsymbol{z} = -\vec{J} \tag{6}$$

$$\mathrm{B} = \sqrt{B_x^2 + B_y^2 + B_z^2} \tag{7}$$

In the equation, B_x, B_y, and $B_z$are the respective components of the magnetic flux density in the *x*, *y*, and *z* directions, respectively.

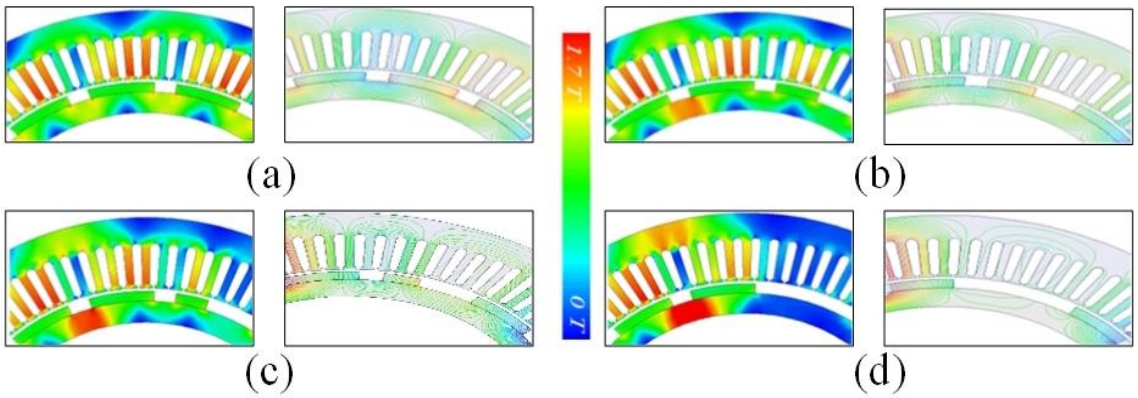

Figure 5. Magnetic flux density distribution: a) healthy model, b) 1/3 broken structure, c) 1/2 broken structure, and d) all broken.

Considering the magnetic flux densities and flux paths, as expected, the fluxes in the stator teeth decreased in the regions where the magnet was broken. Since there was no flux source in the regions where the magnet was broken and reluctance increased, the flux was directed toward the other parts, and an operation close to partial saturation was observed. The torque values of the generator were obtained at rated load and are given in Table 4.

Table 4. Rated torque of design

Model	**Torque** (Nm)
Healthy	63.4167
1/3 demagnetization	59.7818
1/2 demagnetization	57.9554
1 pole demagnetization	53.2662

In permanent magnet machines, torque is formed by the interaction of the stator windings and magnets in the rotor. The magnet area and material affect the magnitude of this torque. When the amount of magnet used decreases, the torque value also decreases [44]. While the torque obtained in the healthy state was 62.5841 N m, it was obtained as 53.2662 N m when one magnet was completely demagnetized. The average torque decreased as the amount of breakage of the magnet increased. There is a 14.88% torque variation between the demagnetized state of a complete magnet and the healthy state. The average torque decreased as the magnetic flux weakened and the distance between the magnets increased. Demagnetization fault also disrupts the distribution of the air gap magnetic flux density. The air gap flux waveform obtained on the contour drawn in the air gap is given in Fig. 6. Fig. 6 clearly shows the

healthy state of a magnet and its effect in the demagnetized state at different rates. The width of the flux waveform of the healthy magnet is equal at all poles in the contour covering the three poles. There is a narrower flux waveform in the structure with 33% breakage and an even narrower flux waveform in the structure with 50% breakage. As expected, the incomplete magnet also has low flux, supporting Fig. 5.

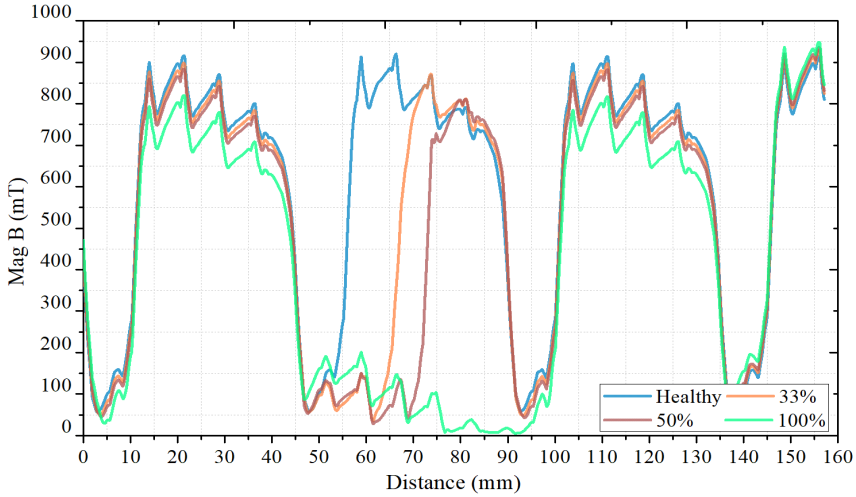

Figure 6. Airgap magnetic flux density waveform.

The induced voltage in generator windings is a function of the magnetic flux within the air gap. Therefore, the air gap's waveform and value affect the magnitude of the induced voltage. Voltage waveforms for Phase *A* in rated load, conducted in transient analyses, are provided in Fig. 7.

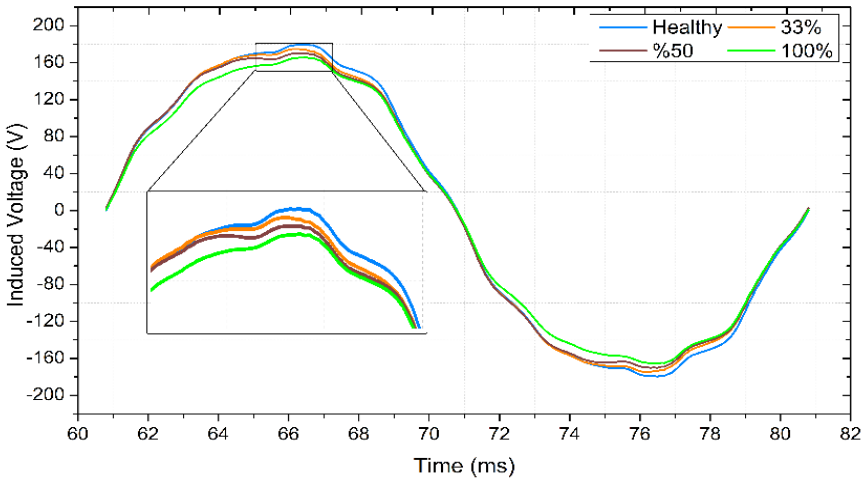

Figure 7. Variation of induced voltage of phase A.

The RMS voltage values of the Phase *A* given in Fig. 7 are provided in Table 5. As expected, due to the decreasing flux, both the peak and effective values of the induced voltage have decreased. Also, the reduction in the total amount of used magnet has led to a decrease in both voltage and torque values.

Table 5. Induced voltage of design.

Model	**Induced voltage** (V)
Healthy	132.1508
1/3 demagnetization	129.4170
1/2 demagnetization	127.3109
1 pole demagnetization	121.8815

5. CONCLUSION

Different types of generators are used in wind turbines. Among these, permanent magnet generators offer the advantage of high torque density and high efficiency. In permanent magnet machines, the material and geometry of the magnet impact the machine's performance. The study explored the performances of a magnet belonging to one pole of the PMSG for different demagnetization rates. Flux waveforms were acquired on the contour drawn in the air gap. When the amount of demagnetization increased, it was observed that the flux became narrower both on the contour and the stator teeth. When the demagnetization amount of the magnet increased, the rated torque and induced voltage value decreased.

Acknowledgment

The short form of the work was presented at the 11th European Conference on Renewable Energy Systems held in Riga/Lithuania on 18-20 May 2023.

REFERENCES

[1] Olabi, AG, Abdelkareem, MA. Renewable energy and climate change. *Renewable and Sustainable Energy Reviews*. 2022; 158, 112111, DOI: 10.1016/j.rser.2022.112111.
[2] Jiang, Q, Zeng, X, Li, B, Wang, S, Liu, T, Chen, Z, Wang, T, Zhang, M. Time-Sharing frequency coordinated control strategy for PMSG-Based wind turbine. *IEEE Journal on Emerging and Selected Topics in Circuits and Systems* 2022; 12(1): 268-278, DOI: 10.1109/JETCAS.2022.3152796.
[3] Dai, LV. Development of converter configuration and corresponding control strategy for wind turbines using permanent magnet synchronous generator: A Case study. *Journal of Energy Systems* 2022; 6(4): 484-502, DOI: 10.30521/jes.1025810.
[4] Abo-Khalil, AG, Alobaid, M. Optimized Control for PMSG Wind Turbine Systems under Unbalanced and Distorted Grid Voltage Scenarios. *Sustainability* 2023; 15(12):1-21, 9552, DOI: 10.3390/su15129552.
[5] Acosta-Silva, Yd-J, Torres-Pacheco, I, Matsumoto, Y, Toledano-Ayala, M, Soto-Zarazúa, GM, Zelaya-Ángel, O, Méndez-López, A. Applications of solar and wind renewable energy in agriculture: A review. *Science Progress* 2019;102(2): 127-140, DOI: 10.1177/0036850419832696
[6] Huang, S, Wang, J, Huang, C, Zhou, L, Xiong, L, Liu, J, Li, P. A fixed-time fractional-order sliding mode control strategy for power quality enhancement of PMSG wind turbine. *International Journal of Electrical Power & Energy Systems* 2022, 134, 107354, DOI: 10.1016/j.ijepes.2021.107354.
[7] Verma P, Misra H, Rajpurohit BS. Design and Analysis of Interior PMSM for Low Power EV Applications in Hilly Terrain. In: IEEE 10th Power India International Conference, New Delhi, India, 25-27 November 2022.
[8] Ruiz-Ponce, G, Arjona, MA, Hernandez, C, Escarela-Perez, R. A Review of Magnetic Gear Technologies Used in Mechanical Power Transmission. *Energies*, 2023; 16(4), 1721, DOI: 10.3390/en16041721.
[9] Nath, AG, Udmale, SS, Singh, SK. Role of artificial intelligence in rotor fault diagnosis: A comprehensive review. *Artificial Intelligence Review* 2021; 54: 2609-2668, DOI: 10.1007/s10462-020-09910-w.
[10] Faiz, J, Nejadi-Koti, K. Demagnetization Fault Indexes in Permanent Magnet Synchronous Motors—An Overview. *IEEE Transactions on Magnetics* 2016; 52(4), 8201511, DOI: 10.1109/TMAG.2015.2480379.
[11] Ruiz, JRR, Rosero, JA, Espinosa, AG, Romeral, L. Detection of Demagnetization Faults in Permanent-Magnet Synchro-nous Motors Under Nonstationary Conditions. *IEEE Transactions on Magnetics* 2009; 45(7): 2961- 2969, DOI: 10.1109/TMAG.2009.2015942.
[12] Rosero JA, Cusido J, Garcia A, Ortega JA, Romeral L. Study on the permanent magnet demagnetization fault in permanent magnet synchronous machines. In IECON 2006-32nd Annual Conference on IEEE Industrial Electronics, Paris, France, 06-10 November 2006, Shanghai, China, 26-28 July 2021, pp. 879-884.
[13] Song, J, Zhao, J, Dong, F, Zhao, J, Xu, L, Yao, Z. A new demagnetization fault recognition and classification method for DPMSLM. *IEEE Transactions on Industrial Informatics* 2020; 16(3): 1559-1570, DOI: 10.1109/TII.2019.2928008.
[14] Ebrahimi, M, Verij Kazemi, M, Gholamian, SA. Detection of partial demagnetization fault in wind turbine permanent magnet generator using a data-driven method. *Electric Power Components and Systems* 2022; 50(9-10): 530-537, DOI: 10.1080/15325008.2022.2136789.

[15] Pietrzak, P, Wolkiewicz, M. Demagnetization Fault Diagnosis of Permanent Magnet Synchronous Motors Based on Stator Current Signal Processing and Machine Learning Algorithms. *Sensors* 2023; 23(4), 1757, DOI: 10.3390/s23041757.
[16] Skowron, M, Orlowska-Kowalska, T, Kowalski, CT. Detection of permanent magnet damage of PMSM drive based on direct analysis of the stator phase currents using convolutional neural network. *IEEE Transactions on Industrial Electronics* 2022, 69(12), 13665-13675, DOI: 10.1109/TIE.2022.3146557.
[17] Skowron M, Kowalski CT. Permanent Magnet Synchronous Motor Fault Detection System Based on Transfer Learning Method. In IECON 2022–48th Annual Conference of the IEEE Industrial Electronics Society, Brussels, Belgium, 17-20 October 2022, pp. 1-6.
[18] Urresty, JC, Riba, JR, Delgado, M, Romeral, L. Detection of demagnetization faults in surface-mounted permanent magnet synchronous motors by means of the zero-sequence voltage component. *IEEE Transactions on Energy Conversion* 2012; 27(1): 42-51, DOI: 10.1109/TEC.2011.2176127.
[19] Ruschetti, C, Verucchi, C, Bossio, G, De Angelo, C, García, G. Rotor demagnetization effects on permanent magnet synchronous machines. *Energy Conversion and Management* 2013; 74: 1-8, DOI: 10.1016/j.enconman.2013.05.001.
[20] Huang, F, Zhang, X, Qin, G, Xie, J, Peng, J, Huang, S, Long, Z, Tang, Y. Demagnetization fault diagnosis of permanent magnet synchronous motors using magnetic leakage signals. *IEEE Transactions on Industrial Informatics* 2023; 19(4): 6105-6116, DOI: 10.1109/TII.2022.3165283.
[21] Sharouni, S, Naderi, P, Hedayati, M, Hajihosseini, P. Demagnetization fault detection by a novel and flexible modeling method for outer rotor permanent magnet synchronous machine. *International Journal of Electrical Power & Energy Systems* 2020;116, 105539, DOI: 10.1016/j.ijepes.2019.105539.
[22] Jia Y, Du Y, Wang Y, Zhang B, Cao W, Ren Y, Li C. Finite Element Simulation on Irreversible Demagnetization of Permanent Magnet Synchronous Generator. In 9th International Conference on Condition Monitoring and Diagnosis, Kita-kyushu, Japan, 13-18 November 2022, pp. 408-412.
[23] Ishikawa, T, Igarashi, N. Failure diagnosis of demagnetization in interior permanent magnet synchronous motors using vibration characteristics. *Applied Sciences* 2019; 9(15), 3111, DOI: 10.3390/app9153111.
[24] Gör, H, Kurt E. Preliminary studies of a new permanent magnet generator (PMG) with the axial and radial flux morphology. *International Journal of Hydrogen Energy* 2016; 41(17): 7005-7018, DOI: 10.1016/j.ijhydene.2015.12.195.
[25] Gör, H, Kurt, E. Effects of Back Iron Components on Efficiency and Generated Power for New Wind Energy Generators, *Electric Power Components and Systems* 2018; 46(10): 1105-1122, DOI: 10.1080/15325008.2018.1488013.
[26] Bouloukza, I, Mordjaoui, M, Kurt, E, Bal, G, Ökmen, C. Electromagnetic design of a new radial flux permanent magnet motor. *Journal of Energy Systems* 2018; 2(1): 13-27, DOI: 10.30521/jes.397836.
[27] İlbaş, M, Demirci, M, Kurt, E. Modeling and experimental validation of flow phenomena for optimum rotor blades of a new type permanent magnet generator. *SN Applied Sciences* 2019; 1, 1544, DOI: 10.1007/s42452-019-1590-1.
[28] Tawfiq, KB, Mansour, AS, Ramadan, HS, Becherif, M, El-Kholy, EE. Wind energy conversion system topologies and converters: Comparative review. *Energy Procedia* 2019; 162: 38-47, DOI:10.1016/j.egypro.2019.04.005.
[29] Polinder, H, Van der Pijl, FF, De Vilder, GJ, Tavner, PJ. Comparison of direct-drive and geared generator concepts for wind turbines. *IEEE Transactions on Energy Conversion* 2006; 21(3):725-733, DOI: 10.1109/TEC.2006.875476.
[30] Özdemir MS, Ocak C, Dalcalı A. Permanent magnet wind generators: neodymium vs. Ferrite magnets. In 3rd International Congress on Human-Computer Interaction, Optimization and Robotic Applications, Ankara, Turkey, 11-13 June 2021, pp. 1-6.
[31] Mahmoud, MM, Salama, HS, Aly, MM, Abdel-Rahim, AMM. Design and implementation of FLC system for fault ride-through capability enhancement in PMSG-wind systems. Wind Eng., 2021;45(5): 1361-1373, DOI: 1 0.1177/0309524X20981773.
[32]Kurt, E, Gör, H, Çelik, K. Optimization of a 3-kW axial flux permanent magnet generator with variable air gap. *International Transactions on Electrical Energy Systems* 2021; 31(11), e13074, DOI: 10.1002/2050-7038.13074.
[33] Upadhyay K.G. Design of electrical machines. New Age International, New Delhi, 2008.
[34] Duan, Y. Method for design and optimization of surface mount permanent magnet machines and induction machines. PhD diss., Georgia Institute of Technology, Atlanta, 2010.
[35] Toliyat HA, Nandi S, Choi S, Meshgin-Kelk H. Electric Machines Modeling, Condition Monitoring, and Fault Diagnosis, CRC Press, Taylor & Francis Group, 2013.
[36] Henao, H, Capolino, GA, Fernandez-Cabanas, M, Filippetti, F, Bruzzese, C, Strangas, E, Pusca, R, Estima, J, Riera-Guasp, M, Hedayati-Kia, S. Trends in fault diagnosis for electrical machines: A review of diagnostic techniques. *IEEE Industrial Electronics Magazine* 2014; 8(2): 31-42, DOI: 10.1109/MIE.2013.2287651.

[37] Strnat, KJ. Modern permanent magnets for applications in electro-technology. Proceedings of the IEEE, 1990, 78(6), pp. 923-946.
[38] Jeong, CL, Hur, J. Optimization design of PMSM with hybrid-type permanent magnet considering irreversible demagnetization. *IEEE Transactions on Magnetics* 2017; 53(11): 1-4, DOI: 10.1109/TMAG.2017.2707102.
[39] Ma, BM, Herchenroeder, JW, Smith, B, Suda, M, Brown, DN, Chen, Z. Recent development in bonded NdFeB magnets. *Journal of Magnetism and Magnetic Materials* 2002; 239(1-3): 418-423, DOI:10.1016/S0304-8853(01)00609-6.
[40] Dalcalı, A, Ocak, C. Effect of Different Magnet Materials on The Performance of Surface Mounted Direct Drive PMSM. *Journal of Awareness*, 2018; 3: 217-224.
[41] Moosavi, SS, Djerdir, A, Amirat, YA, Khaburi, DA. Demagnetization fault diagnosis in permanent magnet synchronous motors: A review of the state-of-the-art. *Journal of Magnetism and Magnetic Materials* 2015; 391: 203-212, DOI: 10.1016/j.jmmm.2015.04.062.
[42] Ebrahimi, BM, Faiz, J. Demagnetization fault diagnosis in surface mounted permanent magnet synchronous motors. *IEEE Transactions on Magnetics* 2013; 49(3): 1185-1192, DOI: 10.1109/TMAG.2012.2217978.
[43] Espinosa, AG, Rosero, JA, Cusido, J, Romeral, L, Ortega, JA. Fault detection by means of Hilbert–Huang transform of the stator current in a PMSM with demagnetization. *IEEE Transactions on Energy Conversion* 2010; 25(2): 312-318, DOI: 10.1109/TEC.2009.2037922.
[44] Faiz, J, Mazaheri-Tehrani, E. Demagnetization modeling and fault diagnosing techniques in permanent magnet machines under stationary and nonstationary conditions: An overview. *IEEE Transactions on Industry Applications* 2017; 53(3): 2772-2785, DOI: 10.1109/TIA.2016.2608950.
[45] Park, Y, Yang, C, Lee, SB, Lee, DM, Fernandez, D, Reigosa, D, Briz, F. Online detection and classification of rotor and load defects in PMSMs based on hall sensor measurements. *IEEE Transactions on Industry Applications* 2019; 55(4): 3803-3812, DOI: 10.1109/TIA.2019.2911252.
[46] Wang, CS, Kao, IH, Perng, JW. Fault Diagnosis and Fault Frequency Determination of Permanent Magnet Synchronous Motor Based on Deep Learning. *Sensors* 2021; 21, 3608, DOI: 10.3390/s21113608.
[47] Dalcalı, A, Akbaba, M. Comparison of the performance of bridge and bridgeless shaded pole induction motors using FEM. *International Journal of Applied Electromagnetics and Mechanics* 2017; 54(3): 341-350, DOI: 10.3233/JAE-160133.
[48] Qi, J, Zhu, Z, Yan, L, Jewell, GW, Gan, C, Ren, Y, Brockway, S, Hilton, C. Influence of Armature Reaction on Electromagnetic Performance and Pole Shaping Effect in Consequent Pole PM Machines. *Energies* 2023; 16(4): 1982, DOI: 10.3390/en16041982.
[49] Gongal, D, Thakur, S, Panse, A, Shankarrao, P, Stark, JA, Hetling, JR, Ozgen, B, Foster, CD. Thermal finite element analysis of localized hypothermia treatment of the human eye. Med. Eng. Phys., 2023; 111, 103928, DOI: 10.1016/j.medengphy.2022.103928.
[50] Moon, J, Chang, H, Lee, J, Kim, CW. Prediction of Internal Circuit and Mechanical-Electrical-Thermal Response of Lithium-Ion Battery Cell with Mechanical-Thermal Coupled Analysis. *Energies* 2022; 15(3), 929, DOI: 10.3390/en15030929.